Superfluid and Dissipative Dynamics of a Bose-Einstein Condensate in a Periodic Optical Potential

S. Burger, F. S. Cataliotti, C. Fort, F. Minardi, and M. Inguscio
INFM-LENS, Dipartimento di Fisica, Università di Firenze, Largo Enrico Fermi 2, I-50125 Firenze, Italia

M. L. Chiofalo and M. P. Tosi
INFM-Scuola Normale Superiore, Piazza dei Cavalieri 7, I-56126 Pisa, Italia
(Received 2 February 2001)

We create Bose-Einstein condensates of ^{87}Rb in a static magnetic trap with a superimposed blue-detuned 1D optical lattice. By displacing the magnetic trap center we are able to control the condensate evolution. We observe a change in the frequency of the center-of-mass oscillation in the harmonic trapping potential, in analogy with an increase in effective mass. For fluid velocities greater than a local speed of sound, we observe the onset of dissipative processes up to full removal of the superfluid component. A parallel simulation study visualizes the dynamics of the Bose-Einstein condensate and accounts for the main features of the observed behavior.

DOI: 10.1103/PhysRevLett.86.4447 PACS numbers: 03.75.Fi, 32.80.Pj, 67.57.De

Bose-Einstein condensates (BEC) in dilute atomic gases are macroscopic quantum systems which can be manipulated by a variety of experimental techniques [1]. The current development of such techniques is opening up a wealth of possibilities to explore new physics, e.g., in nonlinear atom optics [2], and to study various aspects of superfluid behavior in the precisely controllable context of atomic physics [3].

Atoms confined in a periodic potential share some properties with systems of electrons in crystals. Effects known from solid state physics, like Bloch oscillations and Wannier-Stark ladders, have been observed by exposing cold atoms to the dipole potential of far detuned optical lattices [4]. Macroscopic quantum interference has been observed in an experiment on a BEC confined to the antinodes of a far detuned optical lattice [5]. Bragg diffraction from a condensate has been induced in moving optical lattices [6]. This has been used, e.g., as an atom-laser outcoupler [7] and as a tool for spectroscopy of the momentum in BEC's [8]. Applications of BEC's in periodic potentials range from matter-wave transport [9] to interferometry [5] and quantum computing [10]. The question of the stability of the BEC during the evolution in optical potentials is crucial for these applications and has been addressed in theoretical works [11].

In this Letter we report on some novel aspects of superfluidity in BEC's by studying their center-of-mass oscillations inside the harmonic potential of a magnetic trap in the presence of a one-dimensional (1D) optical lattice. We identify different dynamical regimes by varying the initial displacement of the BEC from the bottom of the trap. For small displacements the BEC performs undamped oscillations in the harmonic potential and feels the periodic potential only through a shift in the oscillation frequency. At larger displacements we observe the onset of dissipative processes appearing through a damping in the oscillations. We can describe the experimental results in terms of an inhomogeneous superfluid having a density-dependent critical velocity. In parallel we report numerical studies of the Gross-Pitaevskii equation (GPE), which capture the main features of the observed dynamics.

In our experimental setup [12] we now produce BEC's of ^{87}Rb atoms in the $(F = 1, m_F = -1)$ state. The fundamental frequencies of our Ioffe-type magnetic trap are $\omega_x = 2\pi \times 8.7$ Hz and $\omega_\perp = 2\pi \times 90$ Hz along the axial and radial directions, respectively. The condensates are cigar-shaped with the long axis (the x axis) oriented horizontally. With a number of atoms $N = 4 \times 10^5$, the typical dimensions (Thomas-Fermi radii) are $R_x = 55$ μm and $R_\perp = 5.5$ μm.

We create a 1D optical lattice by superimposing to the long axis of the magnetic trap a far detuned, retroreflected laser beam with wavelength λ. The waist of the beam is 2 orders of magnitude larger than the short condensate axis, and therefore the resulting dipole potential in the condensate region has the form $V(\vec{r}) = V_0 \cos^2(2\pi x/\lambda)$. With a blue detuning $\delta = 2\pi \times 50$ GHz from the D1 line at $\lambda_0 \simeq 795$ nm and an intensity $I = 1$ mW/mm^2 in the antinodes of the standing wave, the dipole potential height of an optical lattice well is $V_0/k_B \simeq 270$ nK [13]. The spontaneous scattering rate in the antinodes is $\Gamma_{\rm sp} \simeq 0.7$ Hz at this detuning and intensity.

To prepare the atomic cloud in the ground state of the combined magnetic trap and optical lattice we first perform evaporative cooling in the magnetic trap until we reach a temperature slightly above the critical temperature, $T \simeq 1.5T_c$. Then we superimpose the optical lattice and continue with the evaporation process down to a temperature $T \simeq T_c/2$, where the thermal cloud is no longer observable. We have checked that the time at which we switch on the optical lattice does affect only the atom number according to the spontaneous scattering rate, but does not influence the BEC dynamics as long as the potential is switched on at a temperature above T_c. It is important

to note that, for the dipole potential strengths and atom numbers which are used in the experiments, the modulated atomic density does not vanish in the antinodes of the lattice but reaches a minimum value which is significantly different from zero.

Figure 1 shows the density distribution along the x axis, as obtained by numerical propagation of the 3D GPE in imaginary time [14]. Here the condensate spans about 250 lattice sites. In the experiment, the density modulation on the length scale of $\lambda/2$ cannot be resolved, due to the limited resolution ($\simeq 7\ \mu$m) of the absorption-imaging system. The modulation on a short length scale raises the chemical potential to the value $\mu/k_B \simeq 170$ nK for $N = 3 \times 10^5$ in the combined trap. Instead, in the purely magnetic trap we have $\mu/k_B \simeq 47$ nK.

In order to investigate the dynamics of the system we translate the magnetic trapping potential in the x direction by a variable distance Δx ranging up to 300 μm by changing the currents through the coils of the magnetic trap. The translation takes a few milliseconds, which is short compared to the longitudinal oscillation period $2\pi/\omega_x$. Therefore, the BEC finds itself out of equilibrium and is subject to a potential gradient which forces it into motion. The presence of the magnetic trapping potential ensures that the atomic cloud maintains its high density (maximum density $n_{\max} \approx 1.5 \times 10^{14}$ cm^{-3}). After an evolution time $t_{\rm ev}$ in the displaced trap, both the magnetic trapping and the optical lattice are switched off simultaneously and the cloud is imaged after an additional free expansion of 26.5 ms. The imaging beam is horizontal and directed perpendicularly to the long condensate axis. From the absorption image we deduce the center-of-mass motion and gain information on the distortion of the BEC.

In the absence of the optical lattice, the center-of-mass motion of the BEC in the displaced trap is an undamped oscillation with frequency $\omega_x = 2\pi \times 8.7$ Hz and amplitude Δx, which in the following we refer to as the "free oscillation." After switching on the optical lattice we observe dynamics in different regimes.

For small displacements, $\Delta x \lessapprox 50\ \mu$m, the dynamics of the BEC resembles the free oscillation at the same amplitude but with a significant shift in frequency. Figure 2 shows a comparison of free oscillations and oscillations with superimposed lattice for $\Delta x = (31 \pm 3)\ \mu$m. For the lattice potential $V_0/k_B \simeq 270$ nK we find a shifted frequency $\omega^* = 2\pi \times (8.0 \pm 0.1)$ Hz. As can be seen from Fig. 2, this frequency shift is also reproduced in numerical simulations of the 1D GPE using an explicit time-marching method [14,15].

The frequency shift can be explained in terms of a renormalization of the atomic mass in the band states originating from the periodic potential. From the data in Fig. 2 we obtain an effective mass $m^*/m = (\omega_x/\omega^*)^2 = 1.18 \pm 0.02$. Different from earlier experiments on cold atoms in an optical lattice under constant acceleration [4], in the present small-amplitude regime under harmonic forces we are exploring only the states near the Brillouin zone center. The above value of m^* refers, therefore, to states near the bottom of the energy band.

The essentially undamped oscillations of the BEC on the time scale of the experiments in the present small-amplitude regime is a manifestation of superfluid behavior. The coherent condensate is being accelerated through band states as if it were a quasiparticle [16]. Also, for small displacements we observe only marginal heating effects; i.e., the small thermal cloud of atoms accompanying the BEC can be fully accounted for by spontaneous scattering.

However, the BEC enters a regime of dissipative dynamics when we further increase the initial displacement Δx and hence the velocity of the condensate. In Fig. 3 we report the measured ratio between the first oscillation peak amplitude and the free-oscillation amplitude as a function of the trap displacement, together with the values from the

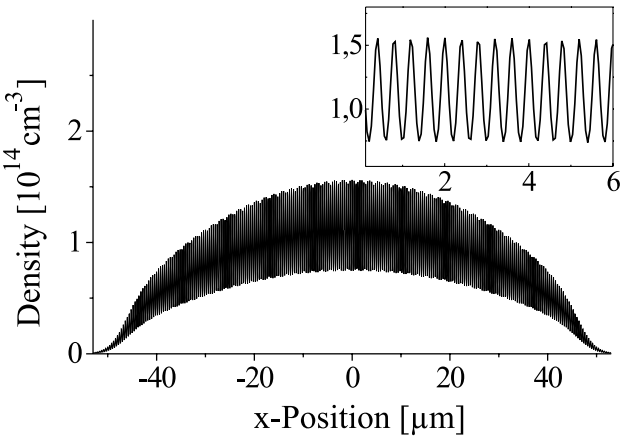

FIG. 1. Density distribution of a BEC in a harmonic trap with a superimposed optical lattice, from a numerical simulation of the 3D GPE for $N = 3 \times 10^5$ and $V_0/k_B = 270$ nK. The inset shows an enlargement of the central region of the BEC. The envelope of the modulated density distribution follows the parabolic distribution in the harmonic trap.

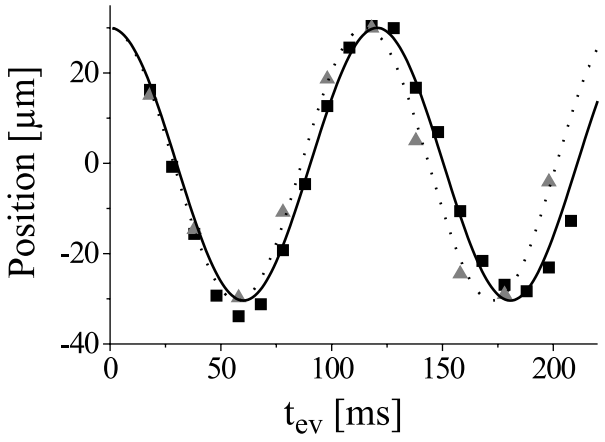

FIG. 2. Superfluid oscillations of a BEC in the presence of an optical lattice potential of height $V_0/k_B \simeq 270$ nK (squares) and in a purely magnetic trap (triangles), for initial displacement $\Delta x = (31 \pm 3)\ \mu$m. The lines give results from a numerical simulation of the 1D GPE at the experimental parameters.

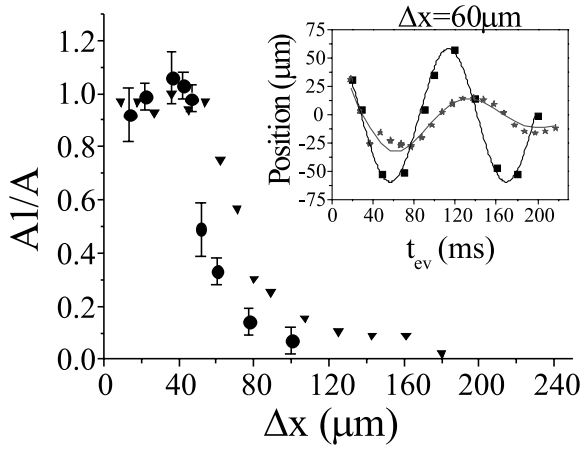

FIG. 3. Ratio of the first-peak amplitude of the oscillation of the ensemble to the free-oscillation amplitude, A_1/A, as a function of initial displacement Δx, for the potential $V_0/k_B \simeq 270$ nK and atom number $N \simeq 3 \times 10^5$. Circles: experimental data; triangles: results from 1D numerical simulation. The inset shows a full oscillation for a displacement $\Delta x = 60$ μm with (stars) and without (squares) optical lattice. Here lines are fits to the data.

numerical simulation. At a displacement $\Delta x \simeq 50$ μm when the maximum velocity attained by the condensate is $v \simeq 3$ mm/s, this ratio suddenly deviates from unity, indicating the insurgence of dissipation in the condensate motion. As shown in the inset of Fig. 3, the subsequent dynamics is a damped oscillation of the center-of-mass at a greatly reduced frequency. The damping increases by further increasing the initial displacement, as is seen in the main body of Fig. 3, this behavior being also displayed by the simulation data in the same figure.

With the onset of dissipative processes the condensate shape in the experiment becomes distorted and a much broader distribution, compatible with a thermal component appears. A thermal component is not allowed to arise in the numerical simulation, which is still based on the GPE. However, the density distribution of the condensate in the simulation becomes fragmented and its phase is completely randomized. That is, the condensate in this regime breaks up into subsystems residing in an essentially independent manner inside the various wells of the periodic potential.

Superfluidity can be expected to disappear when the velocity of flow is sufficient for the spontaneous emission of elementary excitations, as is the case for a homogeneous Bose gas [17]. In a trapped condensate moving at sufficiently high velocities, emission of phonons and other excitations is favored and the gas becomes heated [3,18]. The essentially 1D dynamics of the present sample implies an important role for longitudinal phonon excitations in these processes, with a spectrum of critical velocities because of the inhomogeneity. In a simplified picture, the optical lattice can be viewed as a medium with a microscopic roughness, which leads to a velocity-dependent local compression of the gas moving through the planes of the lattice. This results in a friction force which damps the motion.

Let us therefore inquire about the relative number of atoms in the superfluid component of a BEC in a state of motion at a given velocity v, $N_s(v)/N$ say, with N being the number of atoms inside the harmonic trap in the absence of the optical potential. In order to measure this function and to deduce a maximum critical velocity $v_{\max}$, we have varied the displacement Δx and recorded the atomic distributions after a fixed evolution time $t_{\rm ev} = 40$ ms. For low velocities, up to about 2 mm/s, the sample follows the position of a freely oscillating BEC, the ratio N_s/N being a constant approximately equal to 0.7. This reduction below unity is merely due to the loss of atoms by spontaneous scattering of photons from the optical lattice beams during the preparation of the BEC.

Upon increasing the velocity of the BEC, we observe a retardation of a part of the cloud, leading to a well detectable separation from the superfluid component after free evolution (see inset of Fig. 4). For velocities $v \sim 4$ mm/s we observe that only the central part of the fluid is moving without retardation, leading to a drastically changed aspect ratio with respect to the "unperturbed" BEC. The spatial separation from the thermal component allows a clear demonstration of the superfluid properties of inhomogeneous Bose-Einstein condensates and a precise measurement of the critical velocity. The data for $N_s(v)/N$ in Fig. 4 show a dramatic depletion of the number of atoms in the superfluid component as the velocity of the fluid increases.

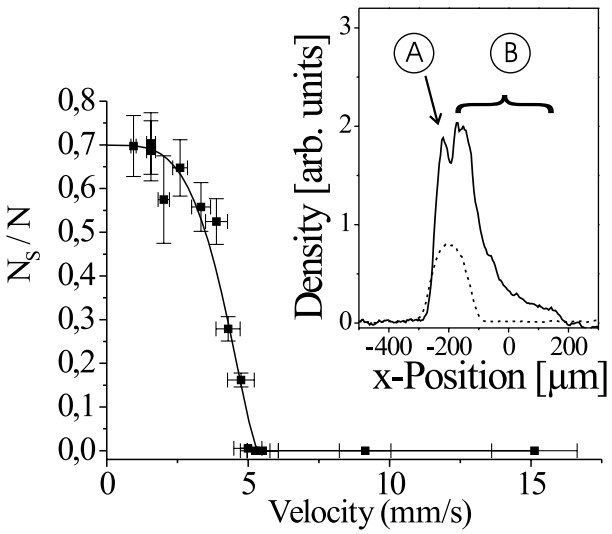

FIG. 4. The fraction of atoms remaining in the undistorted part of the BEC, N_s/N, as a function of the velocity reached during the evolution in the periodic potential. The line shows a fit to the data assuming a 3D parabolic density distribution and a critical velocity proportional to $\sqrt{n(r)}$. In the inset, density distributions as obtained from absorption images of the expanded atomic clouds are represented. Here the solid line shows the density distribution of an ensemble which propagated in the optical lattice at a velocity $v_{\max} \approx 4$ mm/s. The superfluid part (A) appears in the position of a BEC evolving in the absence of the optical lattice (dashed line, rescaled), while the retarded part of the distribution (B) is distributed over a much broader region.

To model the breakdown of superfluidity in the inhomogeneous density distribution of the trapped BEC in Fig. 4, we first discuss the position dependence of the longitudinal sound velocity in the sample. In an inhomogeneous system, as already pointed out by Andrews *et al.* [19] in discussing sound propagation in a magnetically trapped BEC, one may define a local speed of sound $c_s(r)$. This is given by $c_s(r) = \sqrt{(n(r)/m)(\delta\mu/\delta n)}$ [20], where within the Bogoliubov approximation the stiffness constant $\delta\mu/\delta n$ would be equal to the coupling strength g. We have evaluated the appropriate stiffness constant by giving a longitudinal stretching (or squeezing) to our model system by a relative amount ϵ of order 1% at fixed transverse profile. We find $\delta\mu/(\mu\epsilon) \simeq 0.7$. Taking $\mu/k_B \simeq 170$ nK and $\delta n \simeq -n\epsilon$ where n is the average density ($n \simeq 0.4 \times n_{\max} \simeq 6 \times 10^{13}$ cm^{-3}), we find $c_{s,\max} \simeq 5.2$ mm/s for the maximum value of the local sound velocity at the peak of the BEC density. This is in excellent agreement with the data in Fig. 4, showing that complete destruction of the superfluid component occurs at $v_{\max} \simeq 5$ mm/s.

Assuming, therefore, that the critical velocity $v_c(r)$ for local destruction of the superfluid component in the inhomogeneous condensate coincides with the local speed of sound $c_s(r)$, we have $v_c(r) \propto \sqrt{n(r)}$. As observed, superfluidity breaks down first in the low-density regions. The envelope function of the density distribution of the BEC is an inverted parabola in 3D (see Fig. 1) and hence, by integration over the high-density region, we get an equation for the relative number of atoms in the superfluid part of the BEC for a given velocity v, $N_s(v)/N = [5/2 \times (1 - v^2/v_{\max}^2)^{3/2} - 3/2 \times (1 - v^2/v_{\max}^2)^{5/2}]$. This expression implies that about 90% of the atomic probability density is localized in a region which remains superfluid up to velocities $v \simeq v_{\max}/2$. The line in Fig. 4 shows that the above expression for $N_s(v)/N$ gives a very good account of the data, the fitted value of the maximum velocity being $v_{\max} = (5.3 \pm 0.5)$ mm/s.

In further experiments we have also observed indications that the dissipation onset occurs at higher velocities for decreasing V_0 and that the BEC propagates without dissipation in a regime of very low atom number. We plan to investigate these behaviors in detail in future work.

In conclusion, we have investigated the dynamics of BEC's in a periodically modulated potential, in both experimental and numerical simulations. By measuring the effect of the periodic potential on the sloshing-mode oscillation inside the harmonic trap we have determined an average effective mass of the atoms in the condensate. The combined use of a periodic optical potential with the harmonic confinement has allowed us to observe novel features of superfluidity in an inhomogeneous atomic BEC and to demonstrate a new technique for measuring a local density-dependent critical velocity.

The results of this work are of importance for future experiments using periodic potentials for the manipulation of Bose-Einstein condensates and for the understanding of dissipative processes in coherent matter waves. The precise control of the parameters promises to be a powerful tool for a quantitative exploration of novel regimes occurring at different atom numbers or tunnel barrier heights.

We acknowledge discussions with M. Artoni and A. Smerzi and support by the EU under Contracts No. HPRI-CT 1999-00111 and No. HPRN-CT-2000-00125 and by MURST through the PRIN 1999 and PRIN 2000 Initiatives.

[1] See, e.g., *Bose-Einstein Condensation in Atomic Gases,* edited by M. Inguscio *et al.* (IOS Press, Amsterdam, 1999); *Bose-Einstein Condensates and Atom Lasers,* edited by S. Martellucci *et al.* (Kluwer, New York, 2000).
[2] L. Deng *et al.,* Nature (London) **398**, 218 (1999).
[3] C. Raman *et al.,* Phys. Rev. Lett. **83**, 2502 (1999); M. R. Matthews *et al.,* Phys. Rev. Lett. **83**, 2498 (1999); K. W. Madison *et al.,* Phys. Rev. Lett. **84**, 806 (2000); O. M. Maragó *et al.,* Phys. Rev. Lett. **84**, 2056 (2000); A. P. Chikkatur *et al.,* Phys. Rev. Lett. **85**, 483 (2000).
[4] M. Ben Dahan *et al.,* Phys. Rev. Lett. **76**, 4508 (1996); S. R. Wilkinson *et al.,* Phys. Rev. Lett. **76**, 4512 (1996).
[5] B. P. Anderson and M. A. Kasevich, Science **282**, 1686 (1998).
[6] M. Kozuma *et al.,* Phys. Rev. Lett. **82**, 871 (1999).
[7] E. W. Hagley *et al.,* Science **283**, 1706 (1999).
[8] J. Stenger *et al.,* Phys. Rev. Lett. **82**, 4569 (1999).
[9] O. Zobay *et al.,* Phys. Rev. A **59**, 643 (1999); D. Choi and Q. Niu, Phys. Rev. Lett. **82**, 2022 (1999).
[10] D. Jaksch *et al.,* Phys. Rev. Lett. **81**, 3108 (1998); G. K. Brennen *et al.,* Phys. Rev. Lett. **82**, 1060 (1999).
[11] M. L. Chiofalo *et al.,* Eur. Phys. J. D **11**, 371 (2000); A. Trombettoni and A. Smerzi, Phys. Rev. Lett. **86**, 2353 (2001); B. Wu and Q. Niu, e-print cond-mat/0009455, 2000; J. C. Bronski *et al.,* e-print cond-mat/0010099, 2000.
[12] C. Fort *et al.,* Europhys. Lett. **49**, 8 (2000).
[13] We have independently measured the lattice beam intensity by recording the width of an electromagnetically induced transparency window in an absorption line of the BEC.
[14] M. M. Cerimele *et al.,* Phys. Rev. E **62**, 1382 (2000); M. L. Chiofalo *et al.,* Phys. Rev. E **62**, 7438 (2000).
[15] The simulation is carried out on a 1D model after renormalizing the scattering length a to the value $a^* = a(n_{3D}/n_{1D})(\omega_x/\omega_\perp)^{3/2}$, where $n_{3D,1D}$ are the peak densities of the 3D system and of its 1D reduction at the same chemical potential. In the isotropic case this would correspond to setting $\mu_{1D} = \mu_{3D}$. In an elongated system with an essentially frozen transverse dynamics, the effective longitudinal stiffness is reduced by a further factor $(\omega_x/\omega_\perp)^{3/2}$. The longitudinal size of the BEC is approximately preserved by the above 1D reduction.
[16] M. L. Chiofalo *et al.,* Phys. Rev. A (to be published).
[17] D. Pines and P. Nozières, *Theory of Quantum Liquids* (Benjamin, New York, 1966).
[18] Y. Kagan and L. A. Maksimov, Phys. Rev. Lett. **85**, 3075 (2000).
[19] M. R. Andrews *et al.,* Phys. Rev. Lett. **79**, 553 (1997); **80**, 2967 (1998).
[20] G. Baym and C. J. Pethick, Phys. Rev. Lett. **76**, 6 (1996); M. L. Chiofalo *et al.,* Physica (Amsterdam) **254B**, 188 (1998).